DESIGN AND PROTOTYPE PROGRESS TOWARD A SUPERCONDUCTING CRAB CAVITY CRYOMODULE FOR THE APS*

H. Wang#, G. Cheng, C. Ciovati, J. Henry, P. Kneisel, R.A. Rimmer, G. Slack, L. Turlington
Thomas Jefferson National Accelerator Facility, Newport News, VA 23606, USA
G. Waldschmidt, A. Nassiri Argonne National Laboratory, Argonne, IL 60439, USA

Abstract

A squashed, elliptical supercondconducting (SC) cavity with waveguide dampers on the beam pipes has currently been chosen as the baseline design [1] for the Short Pulse X-ray (SPX) project at the Advanced Photon Source (APS). An alternate cavity design, with a waveguide damper located directly on the cavity cell for improved damping characteristics, has also been designed and cold-tested with promising results. In either case, eight cavities would be operated CW in a single cryomodule at 2K to produce an electron bunch chirp of 4MV at a frequency of 2.815 GHz. Detailed analysis of multipactoring (MP), Lorentz force detuning (LFD) and the thermal properties of the baseline design has led to an engineering specification of the basic parameters of the cryomodule.

INTRODUCTION

A scheme has been proposed by Zholents [2] to produce X-ray pulses on the order of picoseconds, using an RF deflecting cavity to chirp the beam to create a quasi-linear correlation between the vertical momentum and the arrival time of the electron bunches. The SC option has been chosen due to its RF power-to-beam voltage efficiency and space requirements for CW operation. A total of 8 cavities, with 0.5 MV deflecting voltage per cavity, are required to chirp the beam, with an additional 8 cavities located downstream to cancel the chirp and revert the bunch to its nominal path.

In order to achieve the required performance, effort has been extended into further prototyping and design analysis for an integrated cryomodule design. The design challenges include high beam current, stringent impedance constraints to ensure coupled bunch stability at 200 mA [3] and transparent operation of the SPX to the remainder of the APS storage ring.

CAVITY PROTOTYPE AND COLD TEST

A prototype of the novel, on-cell damper was built and tested to determine its feasibility for high-gradient operation and multipacting-free performance, see Fig. 1. The on-cell damper prototype was degreased and post-purified at 1200°C for 3 Hrs in a titanium box. Buffered Chemistry Polishing (BCP) was applied for 2x5 minutes with fresh acid (1:1:1), followed by High Pressure Rinsing (HPR) for ~1 hr. The cavity was dried in a class 10 clean room for several hours and then assembled. The waveguide was blanked by a niobium flange and sealed by an indium wire gasket. The assembly was pumped down for several days at room temperature to a 5e-9 mbar vacuum prior to 2K cool.

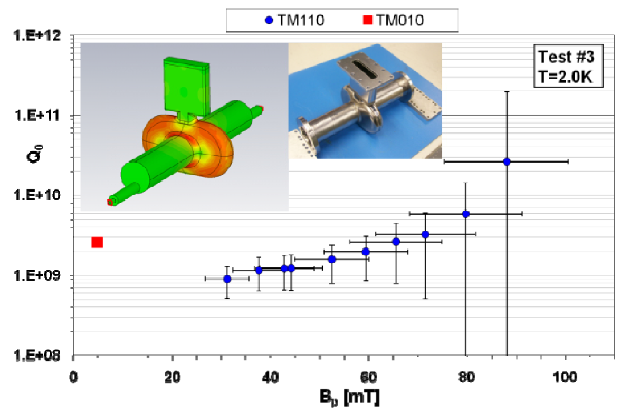

Figure 1: A maximum surface magnetic field of 90 mT in the TM110 mode shown in the left insert has been reached.

The antenna probe, which consisted of a straight copper rod, produced an unreliable electric coupling to the cavity field. It was found that the coupling was sensitive to the rod tilt angle. As a result, an "L"-shaped antenna was constructed, but the rotation angle was not optimal and the coupling was too weak for accurate Q measurements – as shown by the unphysical Q increase in Fig. 1. However, up to 90 mT peak surface magnetic field had been achieved and no sign of multipactoring during the field ramp was observed.

The initial on-cell damper shown in Fig. 1 was made with a narrow slot on the equator in order to perform a proof-of-principle test of the concept. However, a larger opening could increase the surface B-field and limit the achievable gradient of the cavity. In order to improve the damping performance, a dog-bone shape slot was investigated [6] and found to produce enhanced results, as compared with the baseline design (Fig. 6), when two such dampers were used.

A prototype cavity of the baseline design with end-groups is presently being fabricated, see Fig. 2. The lower-order mode (LOM) and higher-order mode (HOM) waveguides were machined by a CNC machine in halves and then electron beam welded together. All walls are made of high RRR niobium, except the beam pipes, which are made of reactor grade, and all flanges are made of NbTi.

* This manuscript has been authored by Jefferson Science Associates, LLC and by UChicago Argonne, LLC under U.S. DOE Contract numbers DE-AC05-06OR23177 and DE-AC02-06CH11357.
#haipeng@jlab.org

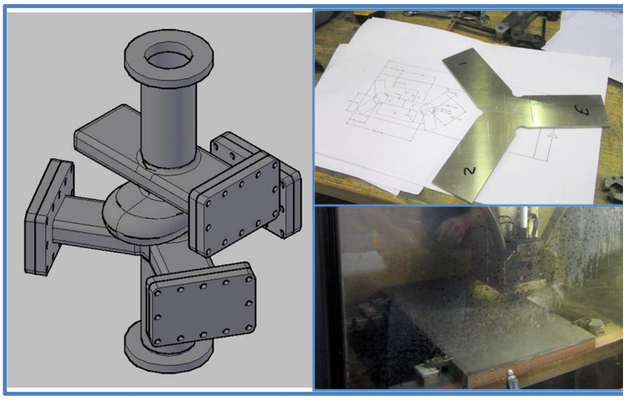

Figure 2: Baseline model (left) for the vertical cold test prototype. EDM wire is cutting (right bottom) on the bulk niobium plate with the "Y" contour for the half waveguide wall. The right, top picture shows the simulated "Y" cut on an aluminum template.

MULTIPACTORING AND LORENTZ FORCE DETUNING

3-D multipactoring simulations were performed on both single-cell structures using Omega3P/Track3P [4], see Fig. 3. The results are similar for both cases which imply that the multipactoring regions are common to both and are not enhanced by the damper design. The most dangerous 2nd order, one-point multipactoring is located near the cavity equator along the squashed surface. The impact energy is approximately 13~18 eV and corresponds to a crabbing voltage level of >0.35 MV and a maximum surface magnetic field of >66.3 mT in the baseline structure. All electrons with a higher impact-energy are associated with higher-order (3~5) multipactoring and are considered less dangerous. Based on experimental benchmarks of other cavity (e.g., a TE011 mode cavity) and the test result in Fig. 1, we believe that the multipactoring of the single-cell cavity designs are not hard limits and can be processed away.

Lorentz force detuning (LFD) was investigated to validate experimental data as well as to consider its effect on the tight phase tolerance required to assure that the SPX system is transparent to the remainder of the APS storage ring. A non-uniform niobium shell thickness of the cavity was shown to cause a large LFD [1], but the addition of waveguide groups reduces this effect.

An LFD value of 22.4-29.8 Hz/(MV/m)^2, depending on structural constraints, was obtained in an ANSYS simulation for the baseline design. At 0.5 MV deflecting voltage, the folded resonance peak, with a loaded Q of 1.2E6, is tilted over its -3dB bandwidth (-1.17 kHz, in Fig. 4). A fast digital self-excited loop control can be used to quickly recover from an RF trip without requiring cavity stiffeners [5].

CRYOSTAT AND COOLING DESIGN

The SPX cavity likely can be integrated into an old

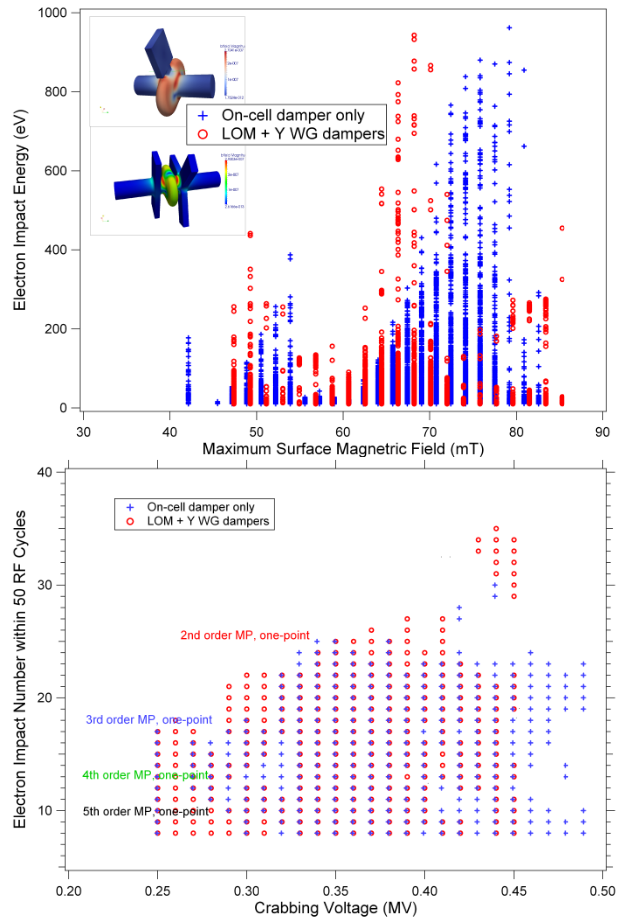

Figure 3: 3-D simulation results of multipactoring in single-cell SPX cavities from Omega3P/Track3P.

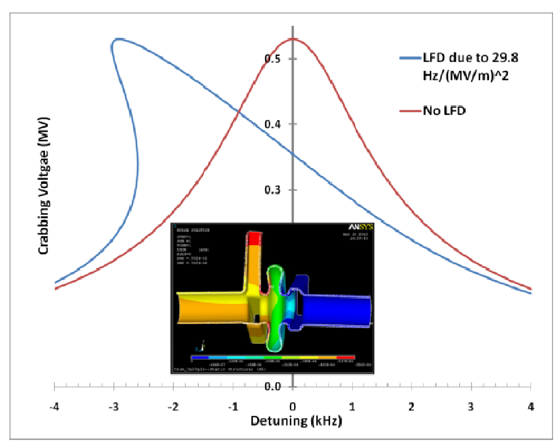

Figure 4: Structural deformation of the baseline SPX cavity due to the Lorentz force (insert) and the resultant detuning of the cavity resonance (blue curve).

CEBAF C100-style helium vessel with only three convolutions of bellows. The end-plates of the helium containment around each cavity could be constructed simply from the waveguide end-groups during fabrication, see Fig. 5. The conductive cooling effect will be confirmed by 3-D RF-thermal simulations.

A 1-D RF-thermal model has been developed to determine the proper Nb flange and 50K heat station locations along the waveguide in order to minimize the heat load to the 2K cryostat. For the nominal case where Bsmax=100 mT, a 0.26W heat load was found where the majority was due to the static heat migrating along the copper coating on the stainless steel waveguide (Fig. 5).

The vertical branch of the "Y" waveguide will be used as a HOM damper as well as the operating mode power coupler. In addition, both low-power [7] and high-power [8] RF load designs have been investigated for LOM and HOM damping.

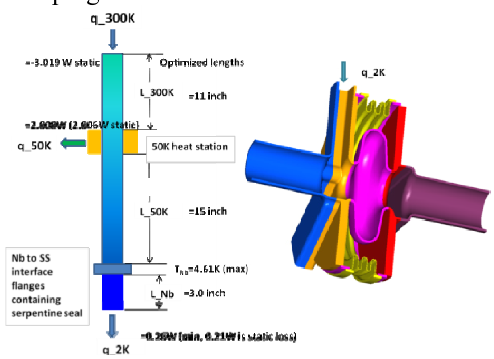

Figure 5: 1-D thermal design optimization with 10 micron Cu coated S.S. waveguide, AlMg seal on Nb flange and a 50K heat station.

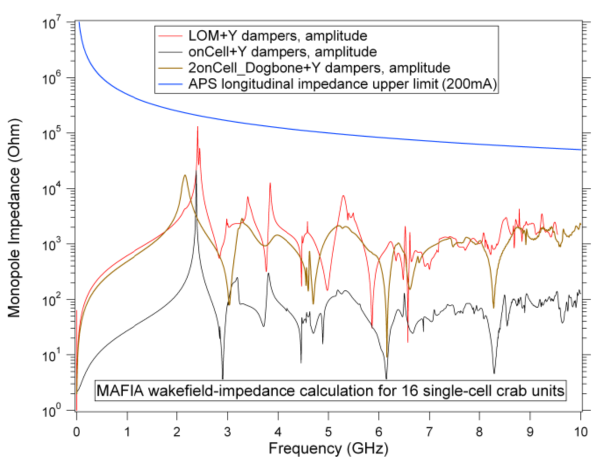

Figure 6: Monopole impedance comparison for three type single-cell damping structures.

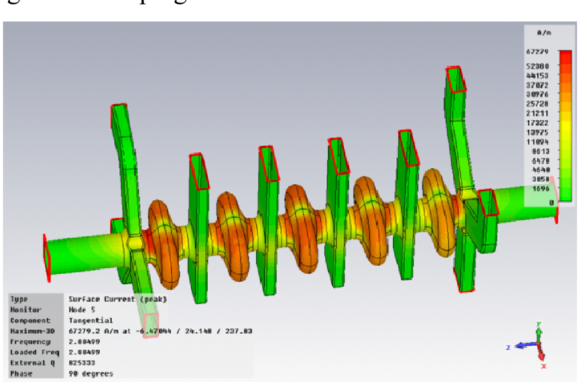

Figure 7: The 5-cell cavity design under the study.

MULTI-CELL OPTION

A 5-cell crab cavity design operating at the "0" mode will improve the cryomodule packing factor, cryogenic efficiency and reduce the waveguide dampers (see Figure 7). Its feasibility and effect on the beam quality is currently under investigation.

CRYOMODULE SPECIFICATION

After systematic R&D, prototyping, simulations and analytical studies of various designs, a final baseline crab cavity design will be chosen by the end of 2010 in order to fully integrate an engineered cryomodule for the SPX project. The major design parameters have been derived and given in Table 1.

Table 1: Main design parameters of SPX cryomodule.

Parameter	Value	Unit
Basline Cavity		
Frequency	2.815488	GHz
Cavity Type	elliptical	
Fundamental Mode	TM110-y-0	vertical kick
Rt/Q including TTF	35.8	Ω
Crabbing Voltage Vt at Bs=100mT	0.53	MV
Peak Surface Bs Field/Vt	195.6	mT/MV
Peak Surface Es Field/Vt	82	1/m
Geometry Factor	227.5	Ω
Material Thickness	3	mm Nb
Cavity Iris Radius	25	mm
Cavity Active Gap Distance	53.24	mm
Operational Q0	>1.0E+09	at 2K
Cell Number	1	
HOM + FPC Couplers	3	"Y" WGs
LOM Coupler	1	WG+stub
TM110-x Mode	3.56	GHz
Lorentz Force Detune (cal. max.)	10.5	kHz/(MV)^2
Tuner Coarse Range, +/-	200	kHz
Tuner Fine Range, +/-	25	kHz
Tuner Fine Resolution	4	Hz, no pieco
Cryomodule		
Operational Crabbing/decrabing Voltage	4	MV
Module Number	2	
Cavity Number per module	8	
Qext, TM110-y-0	1.2E+06	
Klystron Power per Cavity	5	kW
Microphonic Amp. Limit +/- 6σ	100	Hz
Cavity Stiffener	may not need if using fast LLRF	
50K Static Heat Load (FPCs+Shield)	27+180	W
50K Dynamic Heat Load (FPCs+Shield)	76+108	W
2K Static Heat Load per Cavity	2.4	W
2K Dynamic Heat Load per Cavity	7	W
Magnetic Field due to Rebar	<0.1	mT
Axial Magnetric Shielding Factor	>100	
HOM Longitudinal Impedance Upper Limit R (monopole HOMs, Rs=V^2/(2P))	<0.5	MΩ-GHz
HOM Horizontal Impedance Upper Limit Rt (dipole x-HOMs)	<1.4	M Ω/m
HOM Vertical Impedance Upper Limit Rv (dipole y-HOMs)	<7.9	MΩ/m

REFERENCES

[1] H. Wang et al., Proc. PAC 2009, paper WE5PFP059.
[2] A. Zholents et al., NIM A 425, 385 (1999).
[3] Private communication with Y-C. Chae ,Sept, 2007.
[4] https://confluence.slac.stanford.edu/display/AdvComp/ACE3P, SLAC's ACES Suite.
[5] C. Hovater, et al., Proc. PAC 2007, p2481.
[6] J. Shi et al., Proc. EPAC 2008, paper MOPP155.
[7] F. Marhauser, et al., Proc. PAC 2009, paper WE6RFP009.
[8] B. Brajuskovic, et al., Proc. PAC 2007, paper FROBC04.